minerals

MDPI

Article

Mineralogical and Geochemical Characteristics of the Early Permian Upper No. 3 Coal from Southwestern Shandong, China

Xibo Wang [1,*], Lili Zhang [1], Yaofa Jiang [2], Jianpeng Wei [1] and Zijuan Chen [1]

1 State Key laboratory of Coal Resources and Safety Mining, China University of Mining and Technology, Beijing 100083, China; Zhangliliqingdao@gmail.com (L.Z.); weijianpeng15@gmail.com (J.W.); Z.J.Chen94@gmail.com (Z.C.)

2 Jiangsu Institute of Architectural Technology, Xuzhou 221116, China; jiangyaofa-xz@163.com

* Correspondence: xibowang@gmail.com; Tel.: +86-10-6234-1868

Academic Editor: Daniel M. Deocampo

Received: 18 April 2016; Accepted: 16 June 2016; Published: 23 June 2016

Abstract: The Upper No. 3 coal of the Early Permian age is a major workable seam in the southwestern Shandong coalfield, which is located in the eastern part of North China. From Early Jurassic to Neogene, the coalfield was subjected to intensive tectonic processes, leading to a significant rearrangement in depth of coal seams. In this paper, three Upper No. 3 coals occurring at −228, −670 and −938 m in the Luxi, Liangbaosi, and Tangkou mines, respectively, were collected to investigate their mineralogical and geochemical characteristics, with emphasis on modes of occurrence and origin of epigenetic minerals. The three coal seams are similar in vitrinite reflectance, volatile matter yield, and maceral components, suggesting insignificant influence from the tectonic activities on coal rank. Terrigenous minerals (e.g., kaolinite and quartz) are comparable in both types and distribution patterns in the three coals. The presence of siderite and pyrite of syngenetic or penecontemporaneous origin indicate they were emplaced during peat accumulation. The distribution of epigenetic minerals (e.g., calcite, ankerite, and dolomite) are associated with the underground water activities, which were Ca (Mg, Fe)-bearing.

Keywords: coal; tectonic processes; minerals; elements; Early Permian

1. Introduction

Coal mainly consists of organic matter (macerals) and mineral matter (including discrete minerals and inorganic elements) [1,2]. The abundance and modes of occurrences of mineral matter are resulted from processes associated with peat accumulation and rank advance, the interaction of the organic matter with basinal fluids, sediment diagenesis, and in some cases, synsedimentary volcanic inputs [3–7]. Thus minerals in coals provide information about the depositional conditions, geologic history of coal-bearing sequences, and regional tectonic evolution [8–10].

The southwestern Shandong coalfield is located in the eastern part of North China (Figure 1). After the Carboniferous-Permian periods, the southwestern Shandong area was subjected to four episodes of tectonic processes: (1) crustal uplift to Jurassic; (2) fold extrusion deformation during Jurassic and Early Cretaceous; (3) extensional deformation during the Early Cretaceous and Oligocene periods, a stage that can further be separated into the North-South rift stage (Jurassic to Paleocene) and West-East rift stage (Eocene to Oligocene); and (4) post-Neogene subsidence [11]. After the third tectonic activity, graben and horst structure developed in the study area, which resulted in rearrangement of the coal-bearing strata at specific depths [11] (e.g., the Upper No. 3 coals in the Luxi, Liangbaosi, and Tangkou mines occur at various depths of −228, −670 and −938 m, respectively, Figure 1).

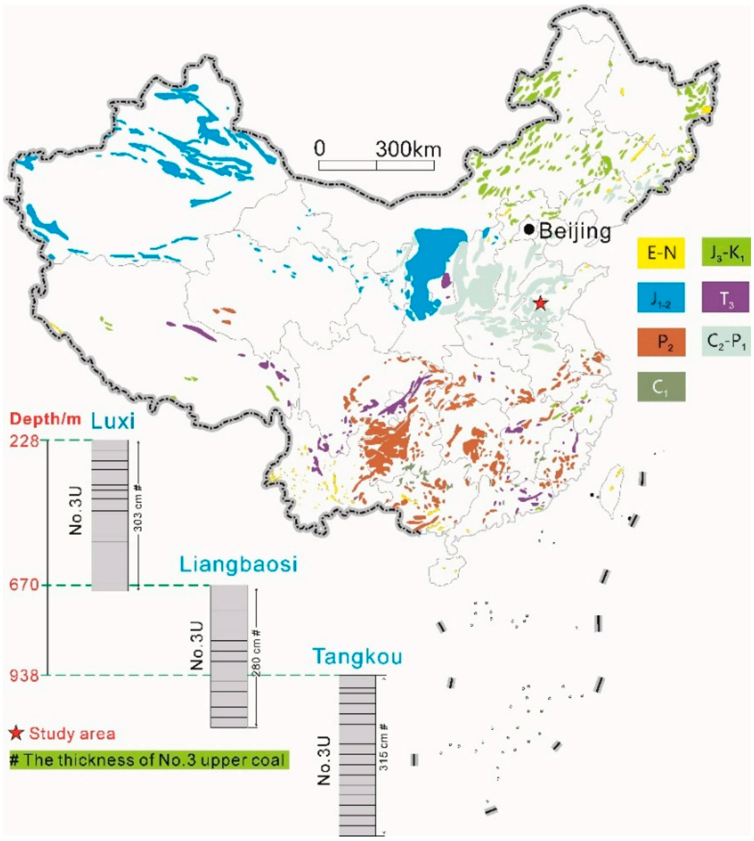

Figure 1. Location of the southwestern Shandong coalfield and the three studied Upper No. 3 coals at various depths.

Differences among maceral, mineral and elemental components between the Carboniferous and Permian coals of the southwestern Shandong coalfield were investigated by Zeng et al. [12] and Liu et al. [13,14]. Distributions and modes of occurrences of As, Se, and Hg in the coal from the Xinglongzhuang mine of the coalfield were also discussed in detail [15]. However, few publications have compared the differing mineralogical and geochemical characteristics of the Upper No. 3 coal at various depths. In the current study, new data on the petrology, mineralogy and geochemistry of the Upper No. 3 coal from the Luxi, Liangbaosi, and Tangkou Mines at various depths were investigate to ascertain the coal characteristics, such as minerals, in addition to major and trace elements.

2. Geological Setting

The Carboniferous-Permian coal deposits mainly occur in North China as shown in Figure 1. The southwestern Shandong coalfield is located in the eastern part of North China. Deposition of the Late Paleozoic coal in North China began with the Benxi Formation of the Late Carboniferous age, and continued into Late Carboniferous to Early Permian Taiyuan, the Shanxi and lower Shihezi Formations, and the upper Shihezi Formation of early Late Permian age. This sequence terminated with non-coal-bearing red clastic strata of the Late Permian Shiqianfeng Formation. The coal-bearing strata of the southwestern Shandong coalfield contain the Taiyuan and Shanxi Formations. The Taiyuan Formation represents a sequence of shallow marine environments, while the Shanxi Formation is of fluvial plain origin. In the study area, the Taiyuan Formation has a thickness of 120–160 m, and consists of siltstone, mudstone, limestone, and coal. The coal in the Taiyuan Formation occurs in up to 18 seams, in which the No. 16 and 17 coals are mineable. The Shanxi Formation has a thickness of 70–100 m, with 2–3 coal seams. The No. 3 coal was divided into upper and lower coal benches by a stable parting, and both benches are workable.

3. Sampling and Methods

The Upper No. 3 coal samples were collected from the Luxi, Liangbaosi and Tangkou mines in the southwestern Shangdong coalfield, China. Due to the rearrangement by tectonic process after coal formation, the burying depth of the No. 3 upper coals in these three mines varies significantly. The coal occurs at −228 m in the Luxi mine, −670 m in the Liangbaosi mine and −938 m in the Tangkou mine, respectively. A total of 43 coal bench samples were collected from the three mines, representing 14 samples from the Luxi mine, 13 from the Liangbaosi mine, and 16 from the Tangkou mine, respectively (Table 1).

Table 1. Moisture, ash yield, volatile matter yield, and total sulfur content (%) in the Upper No. 3 coals from the Luxi, Liangbaosi, and Tangkou mines, southwestern Shandong, China.

Sample	Thickness (cm)	M_{ad}	A_d	V_{daf}	S_d
LX3U-1	20	1.76	10.57	36.24	0.78
LX3U-2	20	1.8	19.43	39.60	1.22
LX3U-4	14	1.91	16.94	35.19	0.72
LX3U-5	30	1.92	9.89	36.46	0.63
LX3U-6	10	2	7.65	38.46	0.82
LX3U-7	17	1.89	10.3	32.24	0.55
LX3U-8	23	1.91	12.99	37.02	0.6
LX3U-10	30	1.69	14.05	35.68	0.5
LX3U-11	15	1.78	10.61	34.77	0.68
LX3U-12	22	1.85	12.32	36.51	0.66
LX3U-13	20	1.86	11.82	34.28	0.86
LX3U-14	40	1.68	11.48	37.00	0.73
LX3U-15	20	1.9	18.54	38.35	0.79
LX3U-16	15	1.92	38.38	45.01	0.9
Luxi *	-	1.83	14.11	36.79	0.73
LBS3U-1	30	1.87	41.39	37.58	1.17
LBS3U-2	20	2.39	8.64	37.19	0.69
LBS3U-3	20	2.02	19.39	37.20	1.17
LBS3U-4	20	2.1	9.04	38.55	0.54
LBS3U-5	20	1.89	6.86	40.12	0.45
LBS3U-6	20	2.05	11.42	35.96	0.32
LBS3U-7	20	2.15	8.45	35.75	0.27
LBS3U-8	20	2.19	8.21	38.22	0.46
LBS3U-9	20	2.05	16.65	38.01	0.37
LBS3U-10	20	2.03	17.52	37.19	0.34
LBS3U-11	30	1.99	10.48	36.85	0.38
LBS3U-12	20	2.13	9.03	33.43	0.43
LBS3U-13	20	1.9	26.03	35.07	0.42
Liangbaosi *	-	2.05	15.65	36.90	0.56
TK3U-1	25	2.07	9	41.63	0.34
TK3U-2	10	2	9.51	36.62	0.51
TK3U-3	20	1.9	7.95	40.01	0.34
TK3U-4	20	2.07	6.42	39.06	0.36
TK3U-5	20	1.97	22.05	34.97	0.26
TK3U-6	20	1.91	14.06	36.17	0.07
TK3U-7	20	1.94	6.95	36.13	0.1
TK3U-8	20	1.87	7.93	36.99	0.25
TK3U-9	20	1.8	9.02	33.25	0.04
TK3U-10	20	2.02	7.39	30.63	0.41

Table 1. *Cont.*

Sample	Thickness (cm)	M_{ad}	A_d	V_{daf}	S_d
TK3U-11	20	2.06	8.76	34.40	0.18
TK3U-12	20	1.94	18.83	34.56	0.26
TK3U-13	20	1.86	10.63	43.83	0.28
TK3U-14	20	2.02	10.03	41.63	0.14
TK3U-15	20	2.09	8.26	36.62	0.36
TK3U-16	20	1.98	7.73	40.01	0.28
Tangkou *	-	1.97	10.29	36.88	0.25

* Average value; M, moisture; A, ash yield; V, volatile matter yield; S, total sulfur content; ad, air dry basis; d, dry basis; daf, air dry and ash free basis.

Proximate analysis for the determination of moisture, volatile matter, and ash yield was performed in accordance with ASTM Standards D3173-11 [16], D3175-11 [17], and D3174-11 [18], respectively. Total sulfur content was determined following the ASTM standard D3177-02 [19]. The reference for vitrinite reflectance determination was an yttrium-aluminum garnet standard (manufacturer Klein and Becker, Idar-Oberstein, Germany) with a certified reflectance of 0.90% for λ = 546 nm under oil immersion. Macerals were identified using white-light reflectance microscopy under oil immersion and more than 500 particles were counted for each polished pellet. The maceral classification and terminology applied in the current study are based on Taylor et al. [20] and the ICCP System (International Committee for Coal and Organic Petrology), 1994 and 2001 [21,22].

Mineral phases were identified from polished pellets using optical microscopy (Leica DM4500P, Leica Microsystems, Wetzlar, Germany), and by X-ray diffraction (XRD). XRD analysis was performed on a Rigaku D/max 2500pc powder diffractometer (Rigaku, Tokyo, Japan) with Ni-filtered Cu-Kα radiation and a scintillation detector. The diffractogram of the powdered sample was recorded over a 2θ interval of 2.6°–70°, with a step size of 0.02° and 0.3 mm receiving silt.

Samples were crushed and ground to pass 200 mesh (75 μm) for geochemical analysis. Oxides of major elements such as SiO_2, TiO_2, Al_2O_3, Fe_2O_3, Na_2O, K_2O, MgO, CaO, MnO and P_2O_5 in coal ash were determined by X-ray fluorescence (XRF) spectrometry (Thermofisher ARL Advant'XP+, Thermo Fisher Scientific, Waltham, MA, USA). Standard references including ASTM2689, ASTM 2690, and ASTM 2691 were used for calibration of major elements. XRF has an accuracy and precision which deviate by less than 1% from the standard reference values. More details of XRF analysis has been described by Dai et al. [23]. Inductively coupled plasma mass spectrometry (ICP-MS, Thermofisher X series II, Thermo Fisher Scientific), in pulse counting mode (three points per peak), was used to determine trace element concentrations in the samples, except for Hg and F. The ICP-MS analysis and sample microwave digestion program are outlined by Dai et al. [24]. Arsenic and Se were determined by ICP-MS using collision cell technology (CCT) in order to avoid disturbance of polyatomic ions [25]. For ICP-MS analysis, samples were digested using an UltraClave Microwave High Pressure Reactor (Milestone Inc., Shelton, CT, USA). Multi-element standards (Inorganic Ventures: CCS-1, CCS-4, CCS-5, and CCS-6; NIST 2685b and Chinese Standard reference GBW 07114 were used for calibration of trace element concentrations. ICP-MS parameters have an accuracy and precision which deviate by less than 5% from the reference standard values. More details of ICP-MS analysis and its method detection limits for various trace elements were described by Dai et al. [23,24] and Li et al. [25]. Mercury was determined using a Milestone DMA-80 analyzer. Samples are heated to make the evolved Hg selectively captured as an amalgam and then measured by Hg analyzer. The detection limit of Hg is 0.005 μg/g and the relative standard deviation 1.5% [23]. Fluorine was determined by pyro-hydrolysis in conjunction with an ion-selective electrode, following the ASTM method D5987-96 [26]. The detection limit is 10 μg/g. The results of two consecutive determinations carried out in the same laboratory by the same operator using the same apparatus do not differ by more than either 15 μg/g (total fluorine concentration of coal is less than 150 μg/g) or 10% (relative; total fluorine concentration of coal is more than 150 μg/g) [27].

4. Results

4.1. Coal Chemistry

Table 1 shows the proximate analysis and total sulfur content data for the Upper No. 3 coals from the Luxi, Liangbaosi, and Tangkou mines. Being comparable among the three coals, moisture contents are 1.83%, 2.05% and 1.97% (on an air dry basis), respectively. Similarly, volatile matter yield does not show distinct differences among the coals from the three mines, being 36.79%, 36.90% and 36.88% (on a dry ash free basis), respectively. Likewise, vitrinite random reflectances of the three coals are 0.77%, 0.76% and 0.75%, respectively. The maximum ash yield is 15.65% in the Upper No. 3 coal from the Liangbaosi mine, followed by 14.11% in the Luxi Upper No. 3 coal and 10.29% in the Tangkou Upper No. 3 coal. However, total sulfur contents are quite different among these three coals. Samples from the Luxi, Liangbaosi, and Tangkou mines have a total sulfur content of 0.73%, 0.56%, and 0.25%, respectively. Through the three seam sections, the maximum total sulfur value occurs in the bench closest to the roof and the lowest sulfur content is located in the middle bench (Figure 2).

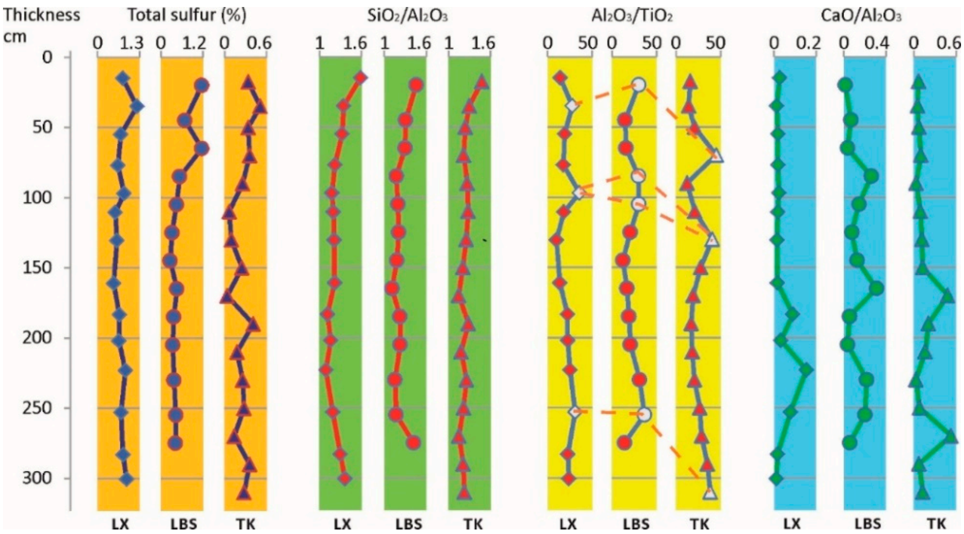

Figure 2. Variations of total sulfur content, the SiO_2/Al_2O_3 ratio, the Al_2O_3/TiO_2 ratio, and the CaO/Al_2O_3 ratio in the profiles of the three Upper No. 3 coals from Luxi (LX), Liangbaosi (LBS), and Tangkou (TK) mines.

4.2. Maceral Compositions

As listed in Table 2, maceral compositions of these three coals are similar, mainly represented by vitrinite, followed by inertinite and liptinite. Total vitrinite contents are 57.9%, 54.7% and 49.5% respectively, which are mainly dominated by collodetrinite (Figure 3A–C,E) and collotelinite (Figure 3C). Total inertinite contents are 29.4%, 32.9% and 35.7%, respectively, and are represented by semifusinite (Figure 3D,F) and macrinite (Figure 3G,H). The inertinite contents of the three Upper No. 3 coals from southwestern Shandong coalfield are higher than those of other Late Paleozoic coal in northern China (generally less than 25% [28]). Nevertheless, the inertinite content in coal present in this study are lower than the inertinite content of the No.6 coal in Jungar Coalfield (including Guanbanwusu [29], Haerwusu [30] and Heidaigou [31] mines), in the northern Ordos Basin in northern China, in which inertinite contents are 56.7%, 53.7%, 37.4%, respectively. The Carboniferous-Permian coals of the Daqingshan coalfield have an inertinite content of 35.3% [32] (Figure 4). Liptinite contents in the three coals present in this study are 12.8%, 11.4% and 14.9%, respectively, and is dominated by sporinite (Figure 5), minor cutinite (Figure 5C,D) and resinite (Figure 5E,F) (Table 2).

Table 2. Maceral compositions of the Upper No. 3 coals from the Luxi, Liangbaosi, and Tangkou mines, southwestern Shandong, China (vol %; on mineral-free basis).

Sample	T	CT	CP	CD	VD	V	Fus	Sfus	Mac	Mic	Fun	ID	I	Sp	Cut	Res	Sub	L
LX3U-1	1.0	13.5	0.7	28.6	1.0	44.7	0.2	8.4	13.7	2.4	0.5	9.9	35.3	14.4	1.0	0.7	3.9	20.0
LX3U-2	1.0	11.7	1.3	39.3	2.9	56.2	0.3	8.4	7.5	0.7	bdl	9.1	25.7	14.0	1.0	bdl	3.3	18.2
LX3U-4	4.3	10.2	0.4	23.6	2.4	40.9	0.4	10.6	13.8	2.4	bdl	15.8	44.1	7.5	2.8	0.4	4.3	15.0
LX3U-5	3.8	12.5	bdl	40.6	0.6	57.5	0.3	5.3	12.8	3.1	bdl	8.1	29.4	9.1	3.4	0.3	0.3	13.1
LX3U-6	2.9	11.2	0.8	51.0	0.4	66.4	0.4	14.5	2.1	1.7	bdl	6.2	24.9	7.1	0.4	0.4	0.8	8.7
LX3U-7	1.6	6.2	bdl	37.7	0.4	45.9	0.4	7.4	18.0	3.7	0.8	4.5	34.4	17.2	0.8	0.4	1.2	19.7
LX3U-8	2.4	16.2	bdl	51.2	1.7	71.5	0.3	5.8	1.7	2.8	bdl	8.9	19.6	8.6	bdl	bdl	0.3	8.9
LX3U-10	0.6	11.7	0.8	36.5	1.4	51.0	0.3	7.2	11.4	2.8	0.8	12.0	34.5	10.3	1.1	0.8	2.2	14.5
LX3U-11	0.7	8.1	bdl	40.0	0.3	49.0	0.3	10.3	12.3	2.3	bdl	10.7	36.5	10.3	0.7	1.0	2.6	14.5
LX3U-12	4.6	8.1	1.6	47.6	0.8	62.7	0.3	3.8	12.4	4.9	0.3	6.2	28.1	7.0	0.8	0.8	0.5	9.2
LX3U-13	3.7	8.3	0.3	41.9	0.3	54.4	0.3	10.1	15.3	2.5	bdl	7.3	36.1	7.3	bdl	0.6	1.5	9.5
LX3U-14	0.7	6.8	0.4	47.0	bdl	54.8	0.4	10.0	11.1	0.7	bdl	9.0	31.2	6.8	0.7	bdl	6.5	14.0
LX3U-15	3.0	14.7	3.0	39.9	9.0	69.6	0.4	4.1	6.8	1.5	bdl	8.7	22.2	2.6	1.1	bdl	4.5	8.3
LX3U-16	7.5	18.4	bdl	29.7	37.9	93.5	0.3	bdl	0.7	1.7	bdl	2.1	4.8	1.4	0.3	bdl	bdl	1.7
Luxi *	2.5	11.0	0.7	40.3	3.4	57.9	0.3	7.4	10.4	2.3	0.2	8.6	29.4	8.8	1.1	0.4	2.5	12.8
LBS3U-1	1.2	28.2	3.5	29.9	5.8	68.4	0.6	4.0	5.2	bdl	bdl	12.1	21.8	6.3	1.7	1.2	0.6	9.8
LBS3U-2	1.0	7.5	0.5	65.0	bdl	74.0	0.5	4.5	2.0	0.5	0.5	4.5	12.5	12.0	0.5	1.0	bdl	13.5
LBS3U-3	0.4	13.5	3.4	50.4	0.8	68.5	0.4	2.1	10.9	0.8	0.4	5.0	20.6	7.1	1.7	0.8	1.3	10.9
LBS3U-4	0.6	10.9	0.3	59.5	bdl	71.3	0.3	6.2	6.9	1.9	0.3	4.7	20.9	5.9	0.6	0.9	0.3	7.8
LBS3U-5	0.6	5.1	0.3	26.6	0.6	33.1	1.5	16.4	21.2	2.7	0.3	7.8	49.9	11.9	1.2	1.8	1.8	17.0
LBS3U-6	3.1	2.8	0.7	49.5	0.4	56.4	0.7	9.3	12.1	1.0	1.0	10.7	35.0	5.2	0.4	2.4	0.7	8.7
LBS3U-7	1.3	1.9	bdl	50.3	bdl	53.5	0.6	7.6	15.9	1.0	bdl	10.8	36.0	6.1	2.6	0.6	1.3	10.5
LBS3U-8	1.0	4.0	0.5	48.5	0.5	54.5	1.0	6.4	17.8	2.0	bdl	5.0	32.2	6.9	bdl	1.0	5.5	13.4
LBS3U-9	1.9	2.3	0.5	38.4	bdl	43.1	bdl	13.4	28.7	1.9	0.5	6.5	50.9	2.3	0.9	1.4	1.4	6.0
LBS3U-10	bdl	0.5	1.0	29.2	bdl	30.6	bdl	12.4	40.2	4.8	bdl	bdl	57.4	4.3	1.0	1.0	0.5	6.7
LBS3U-11	1.5	2.5	bdl	35.6	bdl	39.6	0.5	23.3	23.3	1.0	bdl	bdl	48.0	4.5	2.0	0.5	3.0	9.9
LBS3U-12	2.2	3.9	0.6	51.7	bdl	58.3	0.6	9.4	17.8	2.2	bdl	bdl	30.0	4.4	bdl	1.1	2.8	8.3
LBS3U-13	bdl	1.8	0.6	58.3	bdl	60.7	bdl	6.0	2.4	2.4	bdl	bdl	10.7	19.1	7.1	bdl	0.6	26.8

Table 2. *Cont.*

Sample	T	CT	CP	CD	VD	V	Fus	Sfus	Mac	Mic	Fun	ID	I	Sp	Cut	Res	Sub	L
Liangbaosi *	1.2	7.1	1.0	44.7	0.8	54.7	0.5	9.6	15.6	1.6	0.2	5.2	32.9	7.3	1.5	1.0	1.5	11.4
TK3U-1	0.5	10.4	0.3	38.8	0.8	50.8	0.3	6.5	11.2	3.4	0.3	11.2	32.6	9.1	1.3	1.6	4.7	16.7
TK3U-2	0.7	9.8	0.3	41.7	bdl	52.5	0.3	6.8	10.5	4.8	0.3	10.2	32.9	11.2	1.0	0.3	2.0	14.6
TK3U-3	0.4	2.4	0.7	38.7	bdl	42.2	0.4	11.2	16.4	0.4	bdl	10.1	38.3	13.9	2.1	1.7	1.7	19.5
TK3U-4	0.4	9.9	bdl	51.5	bdl	61.8	0.4	3.9	9.0	2.6	bdl	6.4	21.9	14.2	0.9	0.4	0.9	16.3
TK3U-5	0.3	14.3	bdl	46.1	0.3	61.1	0.3	5.8	13.0	0.7	bdl	5.1	24.6	13.0	0.7	0.7	bdl	14.3
TK3U-6	2.3	12.3	0.3	29.1	1.1	45.0	0.3	12.3	21.1	1.4	0.3	6.0	41.6	12.3	bdl	1.1	bdl	13.4
TK3U-7	0.8	10.6	bdl	36.5	0.4	48.2	0.4	12.2	20.0	1.6	bdl	5.5	40.8	9.0	0.4	0.8	0.4	11.0
TK3U-8	3.1	14.0	bdl	39.3	bdl	56.4	0.4	9.3	14.4	2.0	bdl	5.5	32.3	8.2	0.4	0.4	2.3	11.3
TK3U-9	0.8	9.2	bdl	35.5	bdl	45.4	0.4	11.6	16.3	bdl	bdl	6.4	34.7	12.0	4.4	1.2	2.4	19.9
TK3U-10	0.4	0.8	bdl	34.5	bdl	35.6	0.4	5.7	24.2	0.4	bdl	11.7	42.1	18.2	1.1	2.7	0.4	22.4
TK3U-11	1.2	5.6	bdl	40.6	bdl	47.4	0.4	9.6	19.5	1.6	bdl	4.8	37.1	12.0	0.4	1.2	2.0	15.5
TK3U-12	0.4	4.0	bdl	27.8	bdl	32.1	0.4	7.1	37.3	2.4	0.4	13.5	60.7	4.4	0.4	0.8	1.6	7.1
TK3U-13	1.3	2.3	bdl	34.8	bdl	38.5	0.3	8.0	24.4	0.7	0.3	5.7	39.8	13.7	2.0	1.3	4.7	21.7
TK3U-14	4.1	7.0	bdl	45.6	bdl	56.7	0.4	15.2	13.0	1.5	bdl	1.9	34.4	5.9	bdl	1.5	1.5	8.9
TK3U-15	0.7	6.0	bdl	44.0	bdl	50.7	0.3	9.3	20.0	1.0	0.3	2.3	33.7	11.3	1.7	1.3	1.3	15.7
TK3U-16	0.4	7.3	bdl	60.2	0.7	68.6	0.4	9.1	8.0	0.4	bdl	4.4	22.6	6.9	0.7	0.4	0.7	8.8
Tangkou *	1.1	7.9	0.1	40.2	0.2	49.5	0.4	9.0	17.5	1.5	0.1	6.9	35.7	10.9	1.1	1.1	1.7	14.9

T, telinite; CT, collotelinite; CP, corpogelinite; CD, collodetrinite; VD, vitrodetrinite; V, total vitrinites; Fus, fusinite; Sfus, semifusinite; Mac, macrinite; Mic, micrinite; Fun, funginite; ID, inertodetrinite; I, total inertinites; Sp, sporinite; Cut, cutinite; Res, resinite; Sub, suberinite; L, total liptodetrinite. * Average value; bdl, below detection limit.

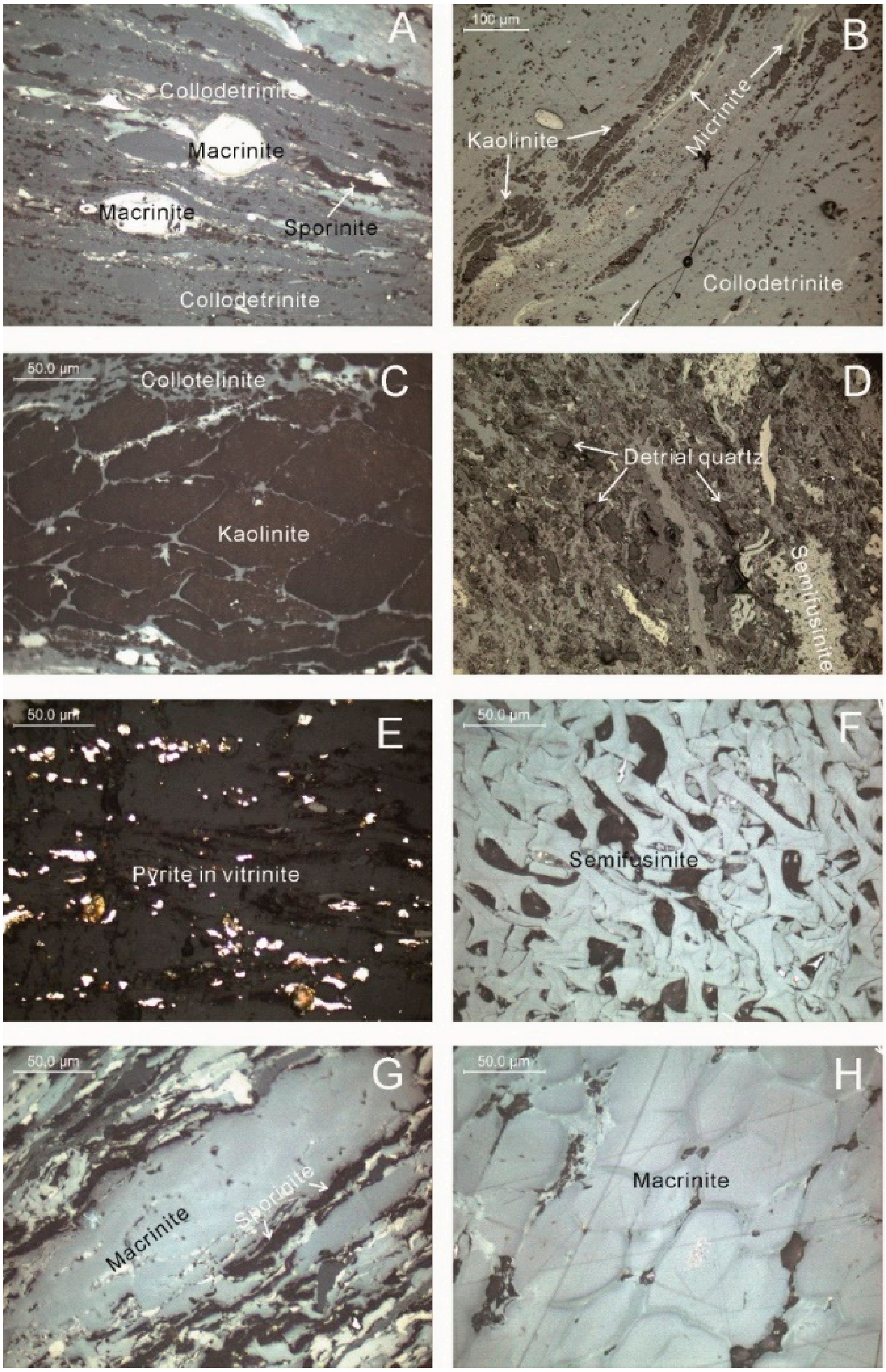

Figure 3. Maceral and minerals in the Upper No. 3 coals. (**A**) Collodetrinite, macrinite, and sporinite (LBS3U-13); (**B**) Kaolinite, micrinite in collodetrinite (LBS3U-8); (**C**) Kaolinite in collotelinite (LBS3U-9); (**D**) detrial quartz grains in macerals (LBS3U-4); (**E**) Pyrite in vitrinite (LBS3U-1); (**F**) Semifusinite; (**G**) Macrinite, Sporinite, and colloderitine (LBS3U-3); (**H**) Macrinite (LBS3U-10). (**A**,**C**–**H**) is under oil reflectance white light; (**B**) is under white reflectance light.

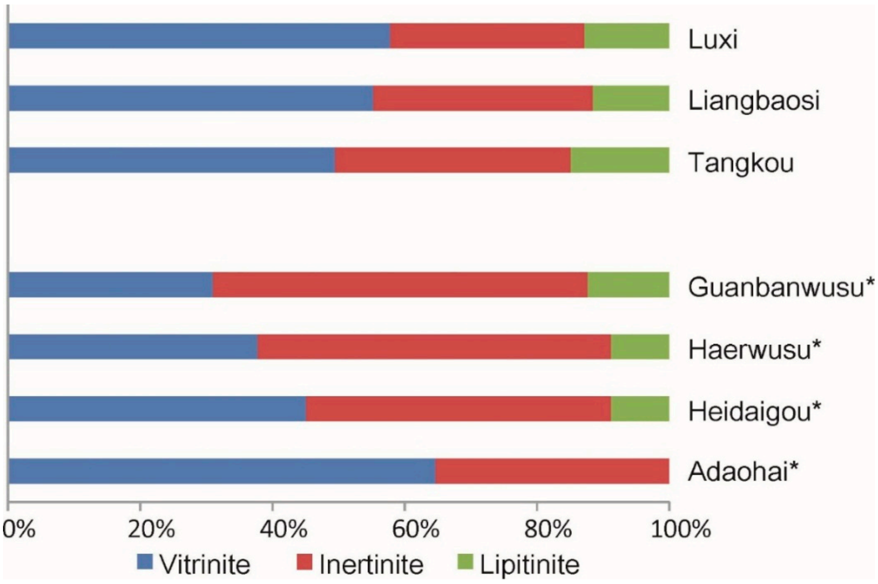

Figure 4. Maceral proportions of the three Upper No. 3 coals from the Luxi, Liangbaosi, and Tangkou mines, as well as the coals from the Guanbanwusu [29], Haerwusu [30], Heidaigou [31], and Adaohai [32] mines.

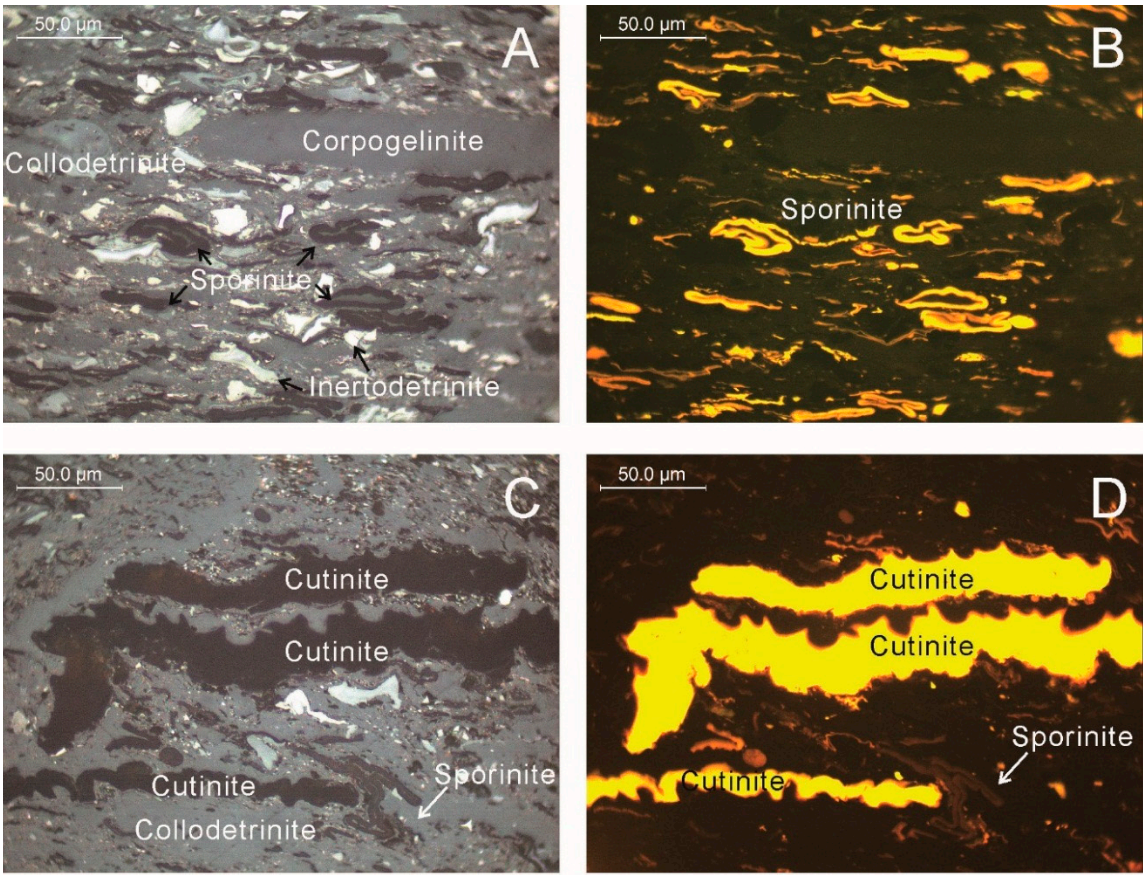

Figure 5. *Cont.*

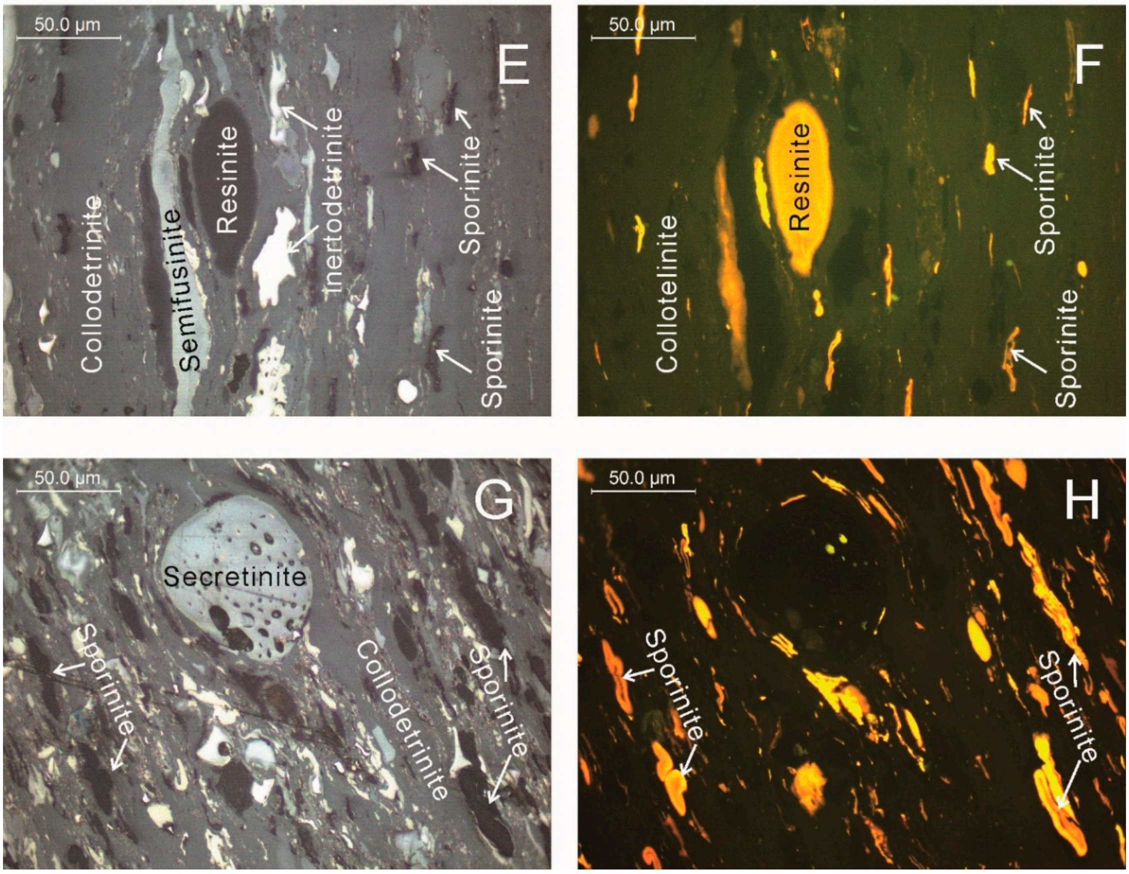

Figure 5. Macerals in the Upper No. 3 coals. (**A**) Sporinite, corpogelinite, inertodetrinite, and colledetrinite (LBS3U-4); (**B**) Sporinite under fluorescent light (LBS3U-4); (**C**) Cutinite, sporinite, and colledetrinite (LBS3U-13); (**D**) Cutinite and sporinte under fluorescent light (LBS3U-13); (**E**) Resinite, inertodetrinite, sporinite, semifusinite and colledetrinte (LBS3U-6); (**F**) Resinite and sporinite under fluorescent light (LBS3U-6); (**G**) Secretinite, sporinite, collodetrinite (LBS3U-4); (**H**) Sporinite under fluorescent light (LBS3U-4). **A**, **C**, **E**, and **G** are under oil reflectance white light.

4.3. Minerals

Minerals identified by XRD in the Upper No. 3 coals are listed in Figure 6. Kaolinite is the most common mineral, with its occurrence observed in each sample present in this study. Mixed layer I/S is prone to occur in the samples close to roof or floor, with exception of the TK3U-12 in Tangkou mine. Chlorite is only detected at the bottom two benches of the Luxi Upper No. 3 coal. The distribution of quartz is similar to that of the mixed layer I/S and is usually most abundant in the samples close to the roof or floor strata. The distribution patterns of siderite and pyrite show a reverse trend through the coal sections. The presence of siderite is much less in the Luxi Upper No. 3 coal than that in Liangbaosi and Tangkou mines. Comparatively, pyrite is common in the Luxi coal and only occurs in the samples close to the roof strata in the Liangbaosi and Tangkou mines. Carbonate minerals including calcite, ankerite, and dolomite are absent in the Luxi coal, but they are present in the Liangbaosi coal. Calcite and ankerite are present in the Tangkou coal samples. Kaolinite occurs as micro beddings (Figure 3B) or lentoid mixed with maceral (Figure 3C). XRD analysis shows that kaolinite in the benches close to the roof or floor is poorly ordered, while kaolinite in the middle benches is well ordered. Other studies reported a similar phenomenon in some coals from the Sydney Basin [33]. Quartz in the Upper No. 3 coals mainly occurs as irregular particles (Figure 3D) within the organic matrix (macerals). Pyrite in the Upper No. 3 coals is present mainly as disseminated fine particles (Figure 3E) or as framboids. Calcite, ankerite, and dolomite are mainly present as fracture-infillings among various macerals.

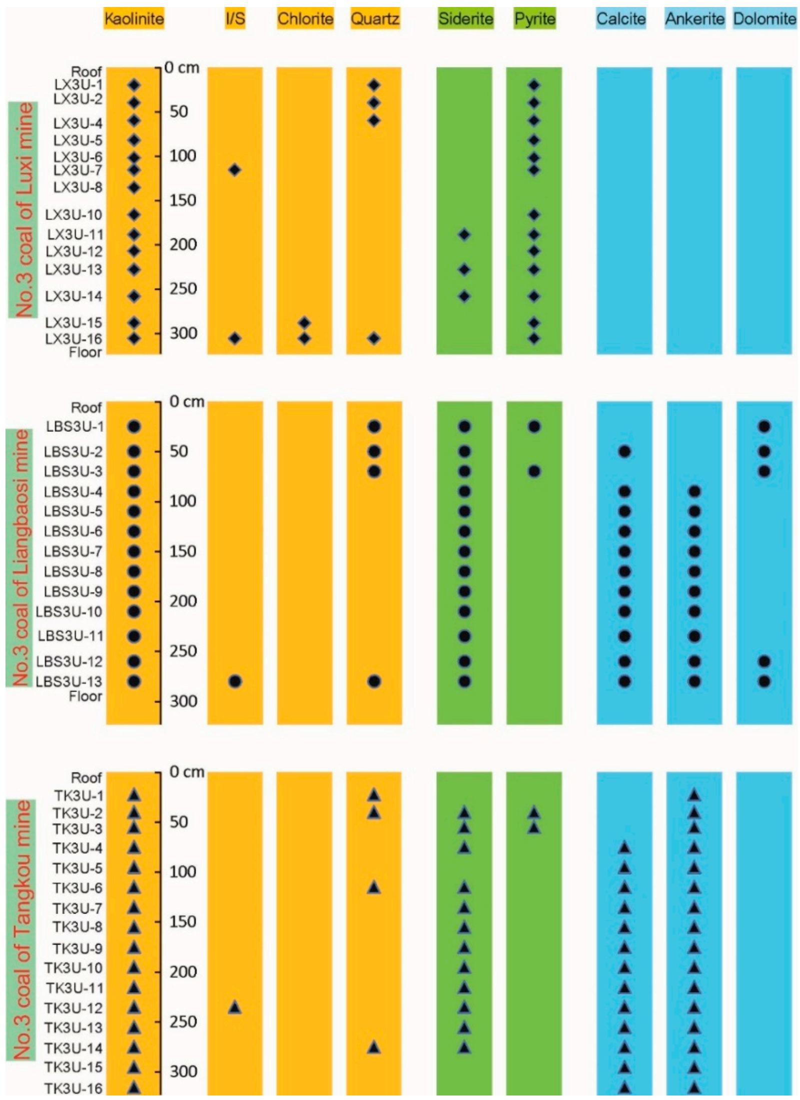

Figure 6. Mineral distributions through the three Upper No. 3 coal sections. I/S, mixed layer illite/smectite.

4.4. Major and Trace Elements

The major element-oxides in the Upper No. 3 coals are SiO_2 and Al_2O_3, followed by CaO, TiO_2, MgO, Fe_2O_3, Na_2O and K_2O (Table 3). Because quartz is absent in most of the Upper No. 3 coal benches, the kaolinite is the major carrier of Si in the coals. In addition to a small proportion of Al in mixed layer I/S, aluminum mainly occurs in the kaolinite. The weight average SiO_2/Al_2O_3 ratios for the Upper No. 3 coals from Luxi, Liangbaosi, and Tangkou mines (1.26, 1.30 and 1.25, respectively) are slightly higher than the theoretical value for kaolinite (1.18) but lower than that for common Chinese coal (1.42), as reported by Dai et al. [34]. The SiO_2/Al_2O_3 ratio distribution patterns through the coal seam sections in the three mines are similar. Particularly, it is lower in the middle portion than in the top or bottom portions. The content of CaO in the Luxi coal (0.2%) is lower than those in the Liangbaosi (0.49%) and Tangkou (0.5%) coals. The positive correlation coefficient between CaO and P_2O_5 (0.98) suggests that CaO is probably associated with apatite in the Luxi coal, although the apatite is too low in content to be detected by XRD technique. The relatively abundant CaO content in the Liangbaosi and Tangkou coals is probably attributed to the epigenetic carbonates (calcite, ankerite, and/or dolomite) deposited from more active underground water.

Table 3. Major element contents (%), the ratios of SiO_2/Al_2O_3, CaO/Al_2O_3, and Al_2O_3/TiO_2 in the Upper No. 3 coals from the Luxi, Liangbaosi, and Tangkou mines, southwestern Shandong, China (%).

Sample	SiO_2	TiO_2	Al_2O_3	Fe_2O_3	MnO	MgO	CaO	Na_2O	K_2O	P_2O_5	SiO_2/Al_2O_3	Al_2O_3/TiO_2	CaO/Al_2O_3
LX3U-1	5.56	0.24	3.50	0.07	0.000	0.05	0.09	0.02	0.05	0.013	1.59	14.43	0.027
LX3U-2	10.37	0.28	7.71	0.25	0.001	0.11	0.09	0.03	0.18	0.017	1.34	27.88	0.012
LX3U-4	8.58	0.34	6.48	0.09	0.001	0.08	0.12	0.03	0.14	0.023	1.32	19.29	0.018
LX3U-5	5.10	0.23	4.17	0.04	0.000	0.04	0.08	0.04	0.03	0.016	1.22	17.80	0.019
LX3U-6	3.68	0.09	3.12	0.04	0.000	0.04	0.07	0.07	0.02	0.011	1.18	35.90	0.023
LX3U-7	5.17	0.23	4.31	0.03	0.000	0.03	0.08	0.08	0.02	0.021	1.20	18.43	0.018
LX3U-8	6.68	0.54	5.52	0.06	0.000	0.06	0.08	0.06	0.04	0.023	1.21	10.16	0.015
LX3U-10	7.10	0.42	5.83	0.07	0.000	0.08	0.09	0.08	0.06	0.037	1.22	13.79	0.016
LX3U-11	4.64	0.18	4.15	0.07	0.000	0.07	0.37	0.12	0.02	0.346	1.12	22.56	0.089
LX3U-12	5.82	0.22	5.01	0.05	0.000	0.05	0.16	0.08	0.02	0.099	1.16	22.70	0.033
LX3U-13	4.90	0.18	4.49	0.07	0.000	0.08	0.69	0.09	0.01	0.514	1.09	25.26	0.154
LX3U-14	6.05	0.16	5.08	0.06	0.001	0.07	0.40	0.09	0.07	0.262	1.19	31.00	0.079
LX3U-15	9.00	0.30	6.93	0.07	0.001	0.13	0.12	0.07	0.24	0.059	1.30	22.91	0.017
LX3U-16	21.18	0.65	15.53	0.45	0.003	0.38	0.17	0.06	0.72	0.024	1.36	23.96	0.011
Luxi *	7.16	0.29	5.69	0.09	0.001	0.08	0.20	0.07	0.10	0.11	1.26	19.66	0.035
LBS3U-1	21.13	0.48	14.53	0.72	0.003	0.28	0.19	0.18	0.49	0.028	1.45	30.16	0.013
LBS3U-2	4.23	0.22	3.24	0.05	0.002	0.08	0.22	0.03	0.03	0.006	1.30	14.93	0.068
LBS3U-3	9.44	0.46	7.29	0.25	0.001	0.13	0.26	0.08	0.08	0.012	1.30	15.89	0.035
LBS3U-4	4.48	0.13	3.83	0.08	0.002	0.13	1.00	0.06	0.02	0.005	1.17	29.95	0.260
LBS3U-5	3.15	0.09	2.63	0.03	0.001	0.08	0.38	0.12	0.03	0.004	1.19	30.28	0.143
LBS3U-6	5.60	0.23	4.64	0.07	0.001	0.12	0.35	0.08	0.04	0.005	1.20	20.60	0.076
LBS3U-7	3.31	0.23	2.81	0.04	0.001	0.10	0.35	0.08	0.02	0.006	1.18	12.33	0.126
LBS3U-8	3.09	0.16	2.79	0.05	0.001	0.13	0.86	0.08	0.01	0.009	1.11	16.99	0.310
LBS3U-9	8.45	0.36	6.90	0.10	0.001	0.12	0.37	0.09	0.06	0.014	1.22	19.15	0.053
LBS3U-10	9.13	0.36	7.45	0.09	0.001	0.10	0.27	0.09	0.04	0.012	1.23	20.68	0.036
LBS3U-11	4.43	0.12	3.85	0.06	0.002	0.13	0.83	0.12	0.03	0.020	1.15	31.07	0.217
LBS3U-12	3.98	0.09	3.40	0.04	0.003	0.08	0.68	0.09	0.03	0.113	1.17	36.56	0.200
LBS3U-13	13.33	0.66	9.40	0.16	0.002	0.20	0.53	0.10	0.40	0.052	1.42	14.19	0.056

Table 3. *Cont.*

Sample	SiO_2	TiO_2	Al_2O_3	Fe_2O_3	MnO	MgO	CaO	Na_2O	K_2O	P_2O_5	SiO_2/Al_2O_3	Al_2O_3/TiO_2	CaO/Al_2O_3
Liangbaosi *	7.61	0.28	5.85	0.15	0.002	0.13	0.49	0.10	0.11	0.02	1.30	21.05	0.083
TK3U-1	4.64	0.20	3.15	0.03	0.001	0.08	0.22	0.03	0.06	0.007	1.47	15.99	0.068
TK3U-2	4.61	0.25	3.55	0.05	0.001	0.08	0.18	0.06	0.05	0.009	1.30	14.26	0.051
TK3U-3	3.78	0.15	3.05	0.04	0.001	0.08	0.22	0.07	0.02	0.007	1.24	20.65	0.072
TK3U-4	3.02	0.06	2.49	0.03	0.001	0.09	0.25	0.04	0.01	0.005	1.22	45.13	0.100
TK3U-5	11.67	0.75	9.21	0.15	0.001	0.16	0.31	0.07	0.07	0.017	1.27	12.33	0.033
TK3U-6	7.13	0.26	5.57	0.08	0.002	0.17	0.53	0.12	0.05	0.012	1.28	21.07	0.094
TK3U-7	3.30	0.06	2.64	0.03	0.001	0.10	0.31	0.12	0.02	0.006	1.25	40.62	0.116
TK3U-8	3.57	0.11	2.97	0.04	0.001	0.11	0.37	0.11	0.02	0.008	1.20	27.60	0.126
TK3U-9	3.56	0.16	3.11	0.05	0.002	0.13	1.49	0.08	0.01	0.012	1.14	19.14	0.481
TK3U-10	3.31	0.15	2.58	0.04	0.001	0.11	0.54	0.06	0.01	0.020	1.28	17.01	0.208
TK3U-11	3.78	0.18	3.21	0.05	0.001	0.15	0.52	0.09	0.02	0.034	1.18	18.20	0.162
TK3U-12	9.96	0.39	7.92	0.14	0.001	0.21	0.24	0.09	0.07	0.015	1.26	20.56	0.030
TK3U-13	5.35	0.17	4.41	0.07	0.003	0.12	0.36	0.07	0.01	0.016	1.22	26.61	0.082
TK3U-14	3.72	0.11	3.24	0.06	0.004	0.16	1.71	0.09	0.01	0.010	1.15	28.63	0.527
TK3U-15	3.91	0.09	3.23	0.03	0.001	0.06	0.24	0.08	0.01	0.008	1.21	35.07	0.073
TK3U-16	3.61	0.08	2.94	0.02	0.001	0.06	0.37	0.06	0.02	0.005	1.23	38.26	0.127
Tangkou *	4.94	0.20	3.95	0.06	0.001	0.12	0.50	0.08	0.03	0.01	1.25	20.22	0.125

* Average value.

Table 4. Concentrations of trace elements in the Upper No. 3 coals from the Luxi, Liangbaosi, and Tangkou mines, southwestern Shandong, China (μg/g unless otherwise indicated).

Sample	Li	Be	F	Sc	V	Cr	Co	Ni	Cu	Zn	Ga	As	Se	Rb	Sr	Zr	Nb	Mo	Cd	Sb	Cs	Ba	REY	Hf	Ta	W	Hg *	Tl	Pb	Bi	Th	U
LX3U-1	29.6	4.4	83.3	7.2	198	14.2	6.2	14.7	37.0	10.8	10.2	1.7	3.8	1.8	57.7	93.4	4.3	4.1	0.5	1.6	0.2	55	48	3.1	0.4	0.5	149	0.2	9.7	0.2	5.0	3.0
LX3U-2	58.9	2.3	73.4	4.3	275	23.5	9.1	19.2	96.9	14.8	11.6	3.1	8.1	7.4	38.1	137	7.7	7.7	0.8	1.2	1.1	60	69	4.8	0.5	0.8	184	0.5	24.8	0.5	5.1	4.8
LX3U-4	61.3	1.8	34.4	7.0	67.3	19.0	3.0	9.0	25.5	9.8	9.7	0.7	5.3	5.8	65.5	154.0	10.1	2.8	0.6	0.5	0.6	73	107	5.6	0.9	1.1	78.6	0.2	16.3	0.4	15.5	3.5
LX3U-5	45.7	0.9	25.8	0.7	31.1	12.5	1.8	5.0	14.8	7.9	6.0	0.7	4.5	0.8	40.4	89.7	6.1	3.3	0.6	0.3	0.1	69	17	3.2	0.6	1.0	85.9	0.1	9.2	0.2	1.9	1.4
LX3U-6	42.4	0.7	30.8	2.0	24.8	9.1	2.6	7.0	12.5	4.7	7.3	0.5	4.3	0.5	66.1	49.2	2.9	4.2	0.4	0.3	0.0	91	83	1.6	0.2	1.5	65.5	0.1	9.9	0.2	3.1	1.1
LX3U-7	61.4	0.9	30.6	3.8	21.3	13.3	1.0	3.8	19.8	9.9	4.5	2.6	5.8	0.7	89.0	86.1	5.1	1.7	0.3	0.1	0.1	116	107	3.1	0.5	0.6	98.2	0.2	9.3	0.2	7.3	1.5
LX3U-8	56.1	0.7	41.0	2.6	54.4	11.9	1.8	4.4	26.3	9.1	8.9	0.8	9.3	1.1	31.4	214	10.8	2.7	0.5	0.4	0.1	82	49	6.6	0.7	0.9	70.1	0.2	21.7	0.3	5.7	2.6
LX3U-10	88.7	1.3	189	7.2	75.6	17.2	1.7	4.5	36.3	17.9	7.5	0.8	9.1	2.1	119	212	8.5	2.2	0.1	0.3	0.2	112	88	6.8	0.6	0.7	136	0.2	18.5	0.3	13.8	3.9

Table 4. *Cont.*

Sample	Li	Be	F	Sc	V	Cr	Co	Ni	Cu	Zn	Ga	As	Se	Rb	Sr	Zr	Nb	Mo	Cd	Sb	Cs	Ba	REY	Hf	Ta	W	Hg *	Tl	Pb	Bi	Th	U
LX3U-11	69.4	1.1	74.0	4.1	48.1	9.3	1.9	3.5	16.9	9.1	6.5	0.9	7.1	0.7	498	131	5.4	2.4	0.4	0.2	0.1	228	173	4.1	0.4	0.4	200	0.1	10.8	0.2	9.2	2.5
LX3U-12	83.3	0.9	431	3.9	39.1	12.0	1.8	4.6	17.7	7.2	6.2	0.7	6.8	0.6	143	101	4.6	3.3	0.3	0.2	0.1	110	55	3.6	0.4	0.9	54.1	0.1	10.5	0.2	5.8	1.6
LX3U-13	90.4	1.3	230	4.0	43.6	13.0	2.0	4.4	15.7	9.8	5.2	0.8	5.4	0.4	572	77.8	4.5	2.7	0.4	0.2	0.0	297	140	2.6	0.3	0.6	121	0.1	8.7	0.2	5.4	1.4
LX3U-14	73.5	1.2	103	4.5	66.0	15.1	2.8	6.9	23.2	7.0	7.6	0.8	6.4	2.4	292	59.0	3.0	3.1	0.3	0.5	0.3	161	105	2.2	0.2	0.8	68.4	0.1	13.5	0.2	4.4	1.9
LX3U-15	93.0	1.4	188	3.9	109	24.5	4.6	10.1	59.9	13.5	11.1	1.6	7.7	12.5	73.7	101	5.8	3.8	0.5	0.9	1.5	101	88	3.7	0.5	0.7	76.6	0.4	22.4	0.5	6.8	2.6
LX3U-16	159	1.4	241	15.1	284	54.0	6.1	17.8	115	28.1	16.2	1.7	7.1	34.0	103	169	9.8	3.9	0.6	0.6	4.3	150	178	6.0	0.8	1.2	72.3	0.6	28.2	0.6	13.6	4.9
Luxi *	71.9	1.4	130	4.8	91.2	17.1	3.2	7.8	35.3	11.2	8.2	1.2	6.6	4.3	160	119	6.2	3.4	0.4	0.5	0.5	122	88	4.1	0.5	0.8	102	0.2	15.1	0.3	7.0	2.6
LBS3U-1	64.8	4.2	53.5	12.1	382	42.9	13.3	24.5	206	52.5	20.8	15.5	7.6	24.3	86.8	173	9.8	5.9	1.0	2.0	5.0	85	396	6.4	0.8	1.8	651	2.3	38.4	0.9	14.4	8.0
LBS3U-2	20.1	3.3	86.9	4.8	71.7	13.1	9.1	12.9	27.5	7.7	9.2	0.7	3.3	1.4	77.5	68.5	5.0	6.0	0.4	1.0	0.2	72	146	2.4	0.4	1.3	105	0.3	10.2	0.3	5.7	2.3
LBS3U-3	52.9	2.7	40.7	4.4	139	18.1	13.3	18.3	54.2	23.5	13.9	5.2	5.2	3.9	72.4	200	16.2	6.2	0.6	1.1	0.6	89	133	7.0	1.4	1.8	718	0.7	19.0	0.5	20.2	4.5
LBS3U-4	20.3	0.7	29.1	1.9	28.5	9.4	5.1	8.4	13.1	6.0	4.7	0.7	3.5	0.5	130	56.8	2.9	3.6	0.3	0.2	0.1	126	63	2.0	0.2	0.7	75.5	0.2	8.6	0.2	3.6	1.0
LBS3U-5	19.1	0.7	36.6	1.5	16.3	6.5	2.3	6.3	8.4	8.8	2.2	0.2	1.9	0.7	98.6	31.7	1.4	1.5	0.4	0.1	0.1	141	49	1.2	0.1	0.5	43.6	0.1	4.5	0.1	2.7	0.5
LBS3U-6	21.5	0.5	31.7	1.5	24.2	10.0	1.9	8.8	8.8	6.5	8.1	0.3	3.5	1.1	61.1	77.9	5.5	1.8	0.5	0.1	0.1	123	65	2.7	0.6	0.5	307	0.1	8.7	0.2	5.2	0.5
LBS3U-7	16.6	0.5	27.4	0.6	15.8	8.8	1.6	7.9	13.1	6.3	3.7	0.3	3.9	0.4	62.1	72.3	3.0	1.4	0.5	0.1	0.0	139	19	2.2	0.2	0.6	130	0.2	4.5	0.1	1.4	0.2
LBS3U-8	28.8	0.4	38.3	1.2	28.5	10.4	1.2	7.7	14.9	11.4	4.2	0.4	3.5	0.4	138	56.5	2.9	1.5	0.2	0.2	0.1	144	27	1.7	0.3	0.6	116	0.2	5.7	0.2	1.1	0.2
LBS3U-9	44.5	0.8	48.0	3.4	40.2	14.5	1.1	6.8	15.3	26.4	15.1	0.2	8.9	1.6	81.8	158	11.8	1.4	0.5	0.3	0.2	135	64	5.4	1.2	1.0	175	0.2	20.3	0.5	11.8	2.3
LBS3U-10	41.7	0.8	37.9	3.6	43.1	15.5	0.7	5.5	19.6	10.2	13.2	0.7	7.9	0.7	56.4	146	8.9	0.9	0.1	0.2	0.1	129	58	4.9	0.9	0.5	207	0.2	19.5	0.5	9.9	0.9
LBS3U-11	50.3	0.6	119	2.4	22.6	9.6	1.4	6.9	9.1	9.7	7.9	0.3	6.2	1.1	205	66.9	3.9	1.5	0.2	0.3	0.1	191	49	2.2	0.3	0.5	137	0.2	10.3	0.2	5.1	1.7
LBS3U-12	38.9	1.1	171	1.3	26.2	29.5	7.1	13.1	9.3	18.0	11.6	0.3	2.8	1.2	211	42.6	2.1	3.8	0.3	0.3	0.1	186	70	1.4	0.2	1.0	117	0.1	8.9	0.1	2.1	0.6
LBS3U-13	41.0	1.5	92.6	4.7	87.2	30.6	9.3	17.1	16.4	24.2	20.1	0.4	8.3	8.0	62.1	269	14.1	2.4	0.5	0.5	1.3	106	64	8.0	1.2	3.2	186	0.3	44.6	0.4	6.6	2.9
Liangbaosi *	37.0	1.4	64.2	3.6	80.5	17.5	5.3	11.4	37.4	17.3	10.6	2.4	5.3	4.1	106	110	6.7	3.0	0.4	0.5	0.7	129	102	3.7	0.6	1.1	240	0.5	16.2	0.3	7.1	2.2
TK3U-1	11.1	3.2	58.0	5.6	121	21.2	5.9	11.3	44.8	10.7	8.4	0.5	5.0	1.4	73.2	95.3	4.8	3.1	0.4	0.7	0.1	100	91	3.0	0.4	1.3	60.9	0.1	13.3	0.3	6.3	2.9
TK3U-2	16.9	1.6	41.2	6.0	179	18.6	4.9	9.8	40.0	7.7	6.8	1.1	5.3	1.5	75.7	75.0	4.7	3.4	0.3	0.5	0.1	117	111	2.4	0.4	0.9	99.1	0.2	12.7	0.2	5.9	2.7
TK3U-3	15.6	1.1	29.8	1.2	85.4	13.5	3.4	7.4	19.0	5.7	4.1	0.8	3.3	0.6	30.3	49.1	3.1	2.7	0.4	0.3	0.0	119	33	1.6	0.3	0.5	68.6	0.1	8.7	0.1	1.9	0.4
TK3U-4	11.6	0.5	65.1	0.7	35.1	9.0	3.4	9.1	13.8	5.1	4.0	0.3	2.6	0.4	28.1	28.9	1.3	3.1	0.4	0.2	0.0	102	39	1.0	0.1	0.9	37.3	0.1	5.2	0.1	1.0	0.2
TK3U-5	29.0	0.5	47.5	4.9	61.3	17.5	2.2	9.7	34.5	14.0	12.6	0.4	7.3	1.6	52.2	237	16.8	2.7	0.4	0.4	0.1	118	111	7.7	1.5	1.4	511	0.2	19.1	0.7	16.7	4.4
TK3U-6	25.0	0.5	31.5	1.1	29.6	14.4	1.7	5.6	14.6	5.9	4.8	0.4	4.1	1.4	22.9	83.2	4.9	1.5	0.4	0.2	0.1	120	22	2.8	0.4	0.7	149	0.1	10.3	0.2	1.6	0.5
TK3U-7	20.7	0.5	43.3	1.3	15.8	7.0	1.5	6.2	7.7	12.1	2.8	0.4	2.3	1.1	96.1	27.4	1.4	1.5	0.5	0.1	0.1	152	53	0.9	0.1	0.3	25.8	0.1	4.9	0.1	2.0	0.5
TK3U-8	20.0	0.6	47.5	1.9	18.4	10.5	1.4	6.7	6.4	6.1	5.3	1.2	4.4	0.7	99.4	43.6	3.9	1.6	0.4	0.1	0.1	146	57	1.5	0.3	0.5	46.8	0.1	8.4	0.1	3.5	0.9
TK3U-9	25.3	0.3	48.6	1.2	11.5	6.2	1.5	6.8	9.9	9.9	3.4	0.4	3.7	0.4	145	47.2	2.1	1.3	0.4	0.1	0.0	173	38	1.6	0.2	0.8	69.2	0.1	4.9	0.1	2.2	0.4
TK3U-10	28.2	0.6	49.7	2.5	13.6	8.6	1.3	6.8	14.4	10.2	2.4	0.5	3.7	0.5	140	44.8	2.2	0.9	0.3	0.1	0.0	183	58	1.5	0.2	0.4	98.3	0.1	3.0	0.1	2.8	0.6
TK3U-11	28.0	0.5	62.3	0.5	17.3	9.7	1.6	7.1	12.0	10.6	3.9	0.2	3.9	0.5	86.1	52.4	2.9	1.0	0.6	0.2	0.0	174	52	1.8	0.2	0.7	238	0.1	6.6	0.2	2.5	0.4
TK3U-12	46.2	1.0	44.9	2.0	27.6	17.2	1.3	8.8	15.1	8.2	9.1	0.0	10.0	1.7	21.6	167	11.7	0.8	0.5	0.2	0.2	109	53	5.8	1.1	0.7	231	0.1	21.2	0.5	10.6	2.5
TK3U-13	52.9	0.9	44.2	3.4	16.4	9.0	2.8	10.9	13.0	9.3	4.5	1.0	4.7	0.6	117	63.6	2.9	0.9	0.3	0.2	0.1	183	90	2.3	0.3	0.5	73.4	0.2	6.5	0.2	6.0	1.3
TK3U-14	34.5	0.7	35.9	2.4	22.9	9.4	4.9	11.8	10.6	9.9	4.1	0.3	3.6	0.7	165	52.2	3.0	1.6	0.4	0.2	0.1	156	70	1.7	0.3	0.6	129	0.1	6.1	0.1	3.8	0.9
TK3U-15	24.2	0.9	44.4	1.6	20.2	11.9	8.2	11.8	10.4	9.8	3.9	0.9	3.4	0.5	47.8	48.2	2.3	1.9	0.5	0.1	0.0	121	58	1.6	0.2	0.7	79.1	0.1	4.0	0.1	3.0	0.4
TK3U-16	18.8	1.7	54.5	4.0	25.8	9.8	8.5	12.3	10.2	13.5	10.1	0.6	3.9	1.0	109	64.8	2.1	2.3	0.7	0.4	0.1	133	64	2.2	0.2	0.8	67.3	0.1	10.4	0.1	3.8	1.3
Tangkou *	25.5	1.0	47.1	2.4	40.7	12.0	3.4	8.9	17.0	9.4	5.6	0.5	4.4	0.9	81.9	74.0	4.4	1.9	0.4	0.2	0.1	138	61	2.5	0.4	0.7	124	0.1	9.0	0.2	4.6	1.2
Word value *	14.0	2.0	82.0	3.7	28.0	17.0	6.0	17.0	16.0	28.0	6.0	8.3	1.3	18.0	100	36.0	4.0	2.1	0.2	1.0	1.1	150	69	1.2	0.3	1.0	100	0.6	9.0	1.1	3.2	1.9

* Average value; Word value from Ketris and Yodovich [35]; Hg as ng/g.

Compared to average values for world hard coals reported by Ketris and Yodovich [35], most trace elements are lower in the Upper No. 3 coal, with the exception of Se, Zr, and Hf which are slightly higher (Table 4, Figure 7). The elevated concentrations of Se, Zr, and Hf have a positive correlation with ash yields, suggesting they were probably associated with the clay mineral (e.g., kaolinite). The enriched Li in the Luxi and Liangbaosi coals may also have similar modes of occurrences. Although the potential hazardous elements As and Hg are overall low in content, they are enriched in some benches. For example, samples LBS3U-1 and LBS3U-3 have high contents of As and Hg, 15.54 μg/g vs. 5.20 μg/g and 651 ng/g vs. 718 ng/g, respectively (Table 4). This is probably a result of their higher total sulfur content of 1.17% and 1.17% (Table 1). The weighted average REY (rare earth elements plus ytrrium [7]) content of the Upper No. 3 coal from the Luxi, Liangbaosi, and Tangkou mines is 88, 102 and 61 μg/g, respectively, close to and lower than the averages for world hard coals (69 μg/g) [35] and Chinese coals (136 μg/g), respectively [34].

Figure 7. Concentration coefficients (CC) of the trace elements in the three Upper No. 3 coals vs. the world hard coal. Data of world hard coals are from Ketris and Yodovich [35]. (**A**) the Luxi Upper No. 3 coal; (**B**) the Luxi Upper No. 3 coal; (**C**) the Tangkou Upper No. 3 coal.

5. Discussion

5.1. Correlation of the Three Upper No. 3 Coals

The tectonic processes rearranged the Upper No. 3 coal at shallow, middle, and deep depths in the Luxi (−228 m), Liangbaosi (−670 m), and Tangkou (−938 m) mines, respectively. Although the studied areas have been subjected to drastic multi-stage tectonic activities, the processes have no or little significant impact on rank, or maceral compositions as described above. Firstly, the three Upper No. 3 coals are comparable in thickness, e.g., 3.03, 2.8 and 3.15 m, respectively. Secondly, the three coals are similar in rank, which is supported by their volatile matter yield (36.79%, 36.90% and 36.88%, respectively) (Table 1) and vitrinite random reflectance (0.77%, 0.76% and 0.75%, respectively), indicating a coal rank of high volatile bituminous (ASTM D388 [36]). Additionally, the maceral components and proportions have no significant differences (Figures 3 and 5).

5.2. Differentiation of Minerals

Minerals in the three Upper No. 3 coals are of terrigenous, authigenic, and epigenetic origins. Terrigenous minerals (e.g., kaolinite and quartz) were attributed to the detrital source during peat accumulating [37]. Authigenic minerals (e.g., pyrite and siderite) were associated with their sedimentary environment during the syngenetic or penecontemporaneous stage of coal formation [38,39]. However, epigenetic minerals (e.g., calcite, ankerite, and dolomite) are related to fluid activities after coalification [37,40].

5.2.1. Terrigenous Minerals

Terrigenous minerals, mainly kaolinite and quartz, share the same distribution patterns through the three coal seam sections, i.e., kaolinite occurs in all the benches and quartz is only present in the benches close to the roof and floor strata. During peat accumulation, the vegetation in and around the mire acted as a filter, preventing quartz particles from penetrating into the mire, while kaolinite is fine enough to be carried into and preserved in the peat mire [37,41]. In the beginning and ending of peat accumulation of the No. 3 coal, the vegetation prevention was weak, thereby allowing quartz particles to be moved into and deposited within the benches close to the floor or roof strata. This explains why the SiO_2/Al_2O_3 ratio is comparable to the theoretical ratio of kaolinite (1.18) in the middle benches but is higher in the upper or bottom benches of the three seam sections (Table 3, Figure 2).

The Al_2O_3/TiO_2 ratio is a valuable provenance indicator of sedimentary rocks [28,29], because the ratio of Al_2O_3 versus TiO_2 in mudstones/sandstones to the same ratio in their parent rocks [42]. The Al_2O_3/TiO_2 ratios is also applied as a provenance indicator for coal and coal-bearing strata [2,40,43–46]. The Al_2O_3/TiO_2 ratios of the Upper No. 3 coals from the Luxi, Liangbaosi, and Tangkou mines are similar in average value (19.66, 21.05, and 20.22, respectively). This is close to the lower end of felsic igneous rocks (21–70) [42]. During Late Carboniferous and Early Permian, the terrigenous source of the coal-bearing basin in North China was dominantly from the northern Yinshan Upland, which is mainly made up of alkaline granite [28]. This is also the case for the Upper No. 3 coal in the southwestern Shandong coalfield, which is supported by the Al_2O_3/TiO_2 ratio.

5.2.2. Authigenic Minerals

Pyrite and siderite are of authigenic origin and they formed syngenetically during peat accumulation [37]. The presence of siderite and pyrite was controlled by the sedimentary environment, where sulfur supply is important because iron in solution would otherwise combine with bacterially produced H_2S instead of reacting with dissolved CO_2, released by fermentation of organic matter [37,47]. The elevated sulfur content (0.73%) is attributed to the common pyrite in the Luxi Upper No. 3 coals, while the lower sulfur content (0.56% and 0.25%) is consistent with a lack of pyrite and frequent presence of siderite in the Liangbaosi and Tangkou coals (Figure 4).

For low sulfur coal (<1% S), sulfur is derived primarily from parent plant material [48]. In medium (1% to <3% S) to high sulfur (⩾3% S) coals, the sulfur is partly inherited from plant and largely from sulfate in seawater that flooded into peat [38,48]. Although the average sulfur content is lower than 1%, the elevated sulfur in the upper benches of the three profiles suggests a seawater influence during the end of the peat accumulation of the Upper No. 3 coal. Chen has reported that the bottom section of Shanxi Formation was subjected to seawater influence [49]. In addition, the variations of sulfur content among the three coals suggest that the seawater influence on the coal-forming peat mire decreases by location, from the Luxi, to the Liangbaosi, and to the Tangkou mine. This is supported by the Sr/Ba ratio in the three coals, 1.31, 0.83 and 0.59, respectively. Because the solubility of Ba compounds is lower than that of Sr, once Ba is precipitated as $BaSO_4$, this compound is difficult to dissolve when sulfate exists in the water [50]. Thus, Sr can move farther seaward than Ba. Therefore, the Sr/Ba ratio is a useful indicator of marine and terrigenous environments, where the ratio increases from terrigenous, paralic, and marine lithofacies [50–52]. The three coals in the present work are different from the Upper No. 3 coal at the Xinglongzhuang mine, southwestern Shandong coalfield. The Xinglongzhuang Upper No. 3 coal has an average sulfur content of 1.49%, with the maximum value occurring in the middle section (3.75%). Pyrite in the coal from the Xinglongzhuang mine occurs mainly as cell or fracture-infillings, with a small proportion of pyrite as disseminated fine particles or framboidal crystals; the sulfur content in the coal from this coalfield is thus attributed to epigenetic invasion as opposed to seawater influence of early diagenesis [15].

5.2.3. Epigenetic Minerals

Calcite in coal is mainly epigenetic origin and occurs as fracture- or cleat-fillings [37]. Detrital calcite is rare in coal because calcite can easily be decomposed under the acidic conditions [53,54]. Occurring as fracture-infillings, carbonate minerals including calcite, ankerite, and/or dolomite in the Upper No. 3 coal are therefore suggestive of an epigenetic origin. They were probably precipitated by circulation of Ca (Mg, Fe)-bearing underground water precipitation [55]. No carbonate minerals are detected in the Luxi coal. However, calcite and ankerite are present in the Liangbaosi and Tangkou coals; dolomite is only present in the Liangbaosi coal (Figure 6). The increase in epigenetic fluids with depth invasion significantly increased the calcium input in the coal. The Luxi coal has a CaO/Al_2O_3 ratio of 0.035, while the same ratio in the Liangbaosi and Tangkou coals is more than double, e.g., 0.083 in the Liangbaosi coal and 0.125 in the Tangkou coal (Table 3, Figure 2). The epigenetic carbonate minerals in coal can be formed in different stages [55–58]. The distribution differences between dolomite and calcite/ankerite suggest that they were not precipitated simultaneously and were probably derived from various fluids with different compositions. Calcite and ankerite were also not from in the same period. For example, the TK3U-1, 2, 3 bench samples in the Tangkou mine have ankerite and no calcite, whereas the sample LBS3U-2 in the Liangbaosi mine has calcite but no ankerite. The current data support that calcite, ankerite, and dolomite in the Liangbaosi coal were derived from various fluids with different compositions and there were at least three stages for epigenetic carbonate mineral precipitation.

6. Conclusions

Due to the tectonic activities after Jurassic, the positions of the Early Permian Upper No. 3 coals were significantly rearranged in depth in the Luxi, Liangbaosi, and Tangkou mines. The three Upper No. 3 coals are similar in rank and maceral compositions, suggesting that there were no significant influences from the tectonic processes. Although the Upper No. 3 coals are low in sulfur, they may still have derived from marine influence. Terrigenous minerals are comparable in both types and distribution patterns among the three coal seam sections; siderite and pyrite signify minerals of syngenetic or penecontemporaneous precipitation origin rather than an epigenetic origin. Epigenetic minerals (e.g., calcite, ankerite, and dolomite) were attributed to invasion by Ca, Mg or Fe-bearing fluids.

Acknowledgments: This research was supported by the National Key Basic Research Program of China (No. 2014CB238900), the National Natural Science Foundation of China (No. 41202121), the Program for Changjiang Scholars and Innovative Research Team in University (IRT13099).

Author Contributions: Xibo Wang conceived the overall experimental strategy and performed major and trace elements measurement. Yaofa Jiang did microscopic experiments. Lili Zhang, Jianpeng Wei and Zijuan Chen did the XRD and coal chemistry analysis. All authors participated in writing the manuscript.

Conflicts of Interest: The authors declare no conflict of interest.

References

1. Ward, C.R. Mineral matter in low-rank coals and associated strata of the Mae Moh basin, northern Thailand. *Int. J. Coal Geol.* **1991**, *17*, 69–93. [CrossRef]
2. Dai, S.; Seredin, V.V.; Ward, C.R.; Hower, J.C.; Xing, Y.; Zhang, W.; Song, W.; Wang, P. Enrichment of U–Se–Mo–Re–V in coals preserved within marine carbonate successions: Geochemical and mineralogical data from the Late Permian Guiding Coalfield, Guizhou, China. *Miner. Depos.* **2015**, *50*, 159–186. [CrossRef]
3. Hower, J.C.; Eble, C.F.; Dai, S.; Belkin, H.E. Distribution of rare earth elements in eastern Kentucky coals: Indicators of multiple modes of enrichment? *Int. J. Coal Geol.* **2016**. [CrossRef]
4. Ward, C.R. Mineralogical analysis in hazard assessment. In *Geological Hazards-the Impact to Mining*; Doyle, R., Moloney, J., Eds.; Coalfield Geology Council of New South Wales: Newcastle, Australia, 2001; pp. 81–88.
5. Ward, C.R.; Corcoran, J.F.; Saxby, J.D.; Read, H.W. Occurrence of phosphorus minerals in Australian coal seams. *Int. J. Coal Geol.* **1996**, *31*, 185–210. [CrossRef]
6. Ward, C.R.; Spears, D.A.; Booth, C.A.; Staton, I.; Gurba, L.W. Mineral matter and trace elements in coals of the Gunnedah Basin, New South Wales, Australia. *Int. J. Coal Geol.* **1999**, *40*, 281–308. [CrossRef]
7. Dai, S.; Graham, I.T.; Ward, C.R. A review of anomalous rare earth elements and yttrium in coal. *Int. J. Coal Geol.* **2016**, *159*, 82–95. [CrossRef]
8. Dai, S.; Ren, D.; Tang, Y.; Yue, M.; Hao, L. Concentration and distribution of elements in Late Permian coals from western Guizhou Province, China. *Int. J. Coal Geol.* **2005**, *61*, 119–137. [CrossRef]
9. Liu, J.; Yang, Z.; Yan, X.; Ji, D.; Yang, Y.; Hu, L. Modes of occurrence of highly-elevated trace elements in superhigh-organic-sulfur coals. *Fuel* **2015**, *156*, 190–197. [CrossRef]
10. Dai, S.; Zeng, R.; Sun, Y. Enrichment of arsenic, antimony, mercury, and thallium in a Late Permian anthracite from Xingren, Guizhou, Southwest China. *Int. J. Coal Geol.* **2006**, *66*, 217–226. [CrossRef]
11. Li, W.C. Workflows of identification of the coalfield tectonic types. *Coal Geol. China* **1998**, *10*, 4–9.
12. Zeng, R.S.; Zhuang, X.G.; Yang, S.K. Quality of the coals from middle area of coal-bearing district of western Shandong. *Coal Geol. China* **2000**, *12*, 10–15.
13. Liu, G.; Yang, P.; Peng, Z.; Chou, C.-L. Petrographic and geochemical contrasts and environmentally significant trace elements in marine-influenced coal seams, Yanzhou mining area, China. *Int. J. Coal Geol.* **2004**, *23*, 491–506. [CrossRef]
14. Liu, G.J.; Zheng, L.G.; Gao, L.F.; Zhang, H.Y.; Peng, Z.C. The characterization of coal quality from the Jining coalfield. *Energy* **2005**, *30*, 1903–1914. [CrossRef]
15. Liu, G.J.; Zheng, L.G.; Zhang, Y.; Qi, C.C.; Chen, Y.W.; Peng, Z.C. Distribution and mode of occurrence of As, Hg and Se and sulfur in coal Seam 3 of the Shanxi Formation, Yanzhou coalfield, China. *Int. J. Coal Geol.* **2007**, *71*, 371–385. [CrossRef]
16. ASTM International. *Test Method for Moisture in the Analysis Sample of Coal and Coke*; ASTM Standard D3173-11; ASTM International: West Conshohocken, PA, USA, 2011.
17. ASTM International. *Test Method for Volatile Matter in the Analysis Sample of Coal and Coke*; ASTM Standard D3175-11; ASTM International: West Conshohocken, PA, USA, 2011.
18. ASTM International. *Annual Book of ASTM Standards. Test Method for Ash in the Analysis Sample of Coal and Coke*; ASTM Standard D3174-11; ASTM International: West Conshohocken, PA, USA, 2011.
19. ASTM International. *Test Methods for Total Sulfur in the Analysis Sample of Coal and Coke*; ASTM Standard D3177-02; ASTM International: West Conshohocken, PA, USA, 2011.
20. Taylor, G.H.; Teichmüller, M.; Davis, A.; Diessel, C.F.K.; Littke, R.; Robert, P. *Organic Petrology*; Gebrüder Borntraeger: Berlin, Germany, 1998; pp. 162–174.

21. International Committee for Coal Petrology (ICCP). The new vitrinite classification (ICCP System 1994). *Fuel* **1998**, *77*, 349–358.
22. International Committee for Coal Petrology (ICCP). The new inertinite classification (ICCP System 1994). *Fuel* **2001**, *80*, 459–471.
23. Dai, S.; Hower, J.C.; Ward, C.R.; Guo, W.; Song, H.; O'Keefe, J.M.K.; Xie, P.; Hood, M.M.; Yan, X. Elements and phosphorus minerals in the middle Jurassic inertinite-rich coals of the Muli Coalfield on the Tibetan Plateau. *Int. J. Coal Geol.* **2015**, *144–145*, 23–47. [CrossRef]
24. Dai, S.; Wang, X.; Zhou, Y.; Hower, J.C.; Li, D.; Chen, W.; Zhu, X. Chemical and mineralogical compositions of silicic, mafic, and alkali tonsteins in the late Permian coals from the Songzao Coalfield, Chongqing. Southwest China. *Chem. Geol.* **2011**, *282*, 29–44. [CrossRef]
25. Li, X.; Dai, S.; Zhang, W.; Li, T.; Zheng, X.; Chen, W. Determination of As and Se in coal and coal combustion products using closed vessel microwave digestion and collision/reaction cell technology (CCT) of inductively coupled plasma mass spectrometry (ICP-MS). *Int. J. Coal Geol.* **2014**, *124*, 1–4. [CrossRef]
26. ASTM International. *Standard Test Method for Total Fluorine in Coal and Coke by Pyrohydrolytic Extraction and Ion Selective Electrode or Ion Chromatograph Methods*; ASTM Standard D5987–96; ASTM International: West Conshohocken, PA, USA, 2011.
27. Dai, S.; Ren, D. Fluorine concentration of coals in China—An estimation considering coal reserves. *Fuel* **2006**, *85*, 929–935. [CrossRef]
28. Han, D.; Ren, D.; Wang, Y.; Jin, K.; Mao, H.; Qin, Y. *Coal Petrology in China*; China University of Mining & Technology Press: Xuzhou, China, 1996. (In Chinese)
29. Dai, S.; Jiang, Y.; Ward, C.; Gu, L.; Seredin, V.; Liu, H.; Zhou, D.; Wang, X.; Sun, Y.; Zou, J.; et al. Mineralogical and geochemical compositions of the coal in the Guanbanwusu Mine, Inner Mongolia, China: Further evidence for the existence of an Al (Ga and REE) ore deposit in the Jungar Coalfield. *Int. J. Coal Geol.* **2012**, *98*, 10–40. [CrossRef]
30. Dai, S.; Li, D.; Chou, C.-L.; Zhao, L.; Zhang, Y.; Ren, D.; Ma, Y.; Sun, Y. Mineralogy and geochemistry of boehmite-rich coals: New insights from the Haerwusu Surface Mine, Jungar Coalfield, Inner Mongolia, China. *Int. J. Coal Geol.* **2008**, *74*, 185–202. [CrossRef]
31. Dai, S.; Ren, D.; Chou, C.-L.; Li, S.; Jiang, Y. Mineralogy and geochemistry of the No. 6 coal (Pennsylvanian) in the Junger Coalfield, Ordos Basin, China. *Int. J. Coal Geol.* **2006**, *66*, 253–270. [CrossRef]
32. Dai, S.; Zou, J.; Jiang, Y.; Ward, C.R.; Wang, X.; Li, T.; Xue, W.; Liu, S.; Tian, H.; Sun, X.; et al. Mineralogical and geochemical compositions of the Pennsylvanian coal in the Adaohai Mine, Daqingshan Coalfield, Inner Mongolia, China: Modes of occurrence and origin of diaspore, gorceixite, and ammonian illite. *Int. J. Coal Geol.* **2012**, *94*, 250–270. [CrossRef]
33. Ward, C.R.; Warbrooke, P.R.; Roberts, I. Geochemical and mineralogical changes in a coal seam due to contact metamorphism, Sydney Basin, New South Wales, Australia. *Int. J. Coal Geol.* **1989**, *11*, 105–125. [CrossRef]
34. Dai, S.; Ren, D.; Chou, C.-L.; Finkelman, R.B.; Seredin, V.V.; Zhou, Y. Geochemistry of trace elements in Chinese coals: A review of abundances, genetic types, impacts on human health, and industrial utilization. *Int. J. Coal Geol.* **2012**, *94*, 3–21. [CrossRef]
35. Ketris, M.P.; Yudovich, Y.E. Estimations of Clarkes for carbonaceous biolithes: World average for trace element contents in black shales and coals. *Int. J. Coal Geol.* **2009**, *78*, 135–148. [CrossRef]
36. ASTM International. *Standard Classification of Coals by Rank*; ASTM Standard D388-07; ASTM International: West Conshohocken, PA, USA, 2011.
37. Ward, C.R. Analysis and significance of mineral matter in coal seams. *Int. J. Coal Geol.* **2002**, *50*, 135–168. [CrossRef]
38. Chou, C-L. Sulfur in coals: A review of geochemistry and origins. *Int. J. Coal Geol.* **2012**, *100*, 1–13. [CrossRef]
39. Dai, S.; Hou, X.; Ren, D.; Tang, Y. Surface analysis of pyrite in the No. 9 coal seam, Wuda Coalfield, Inner Mongolia, China, using high-resolution time-of-flight secondary ion mass-spectrometry. *Int. J Coal Geol.* **2003**, *55*, 139–150. [CrossRef]
40. Johnston, M.N.; Hower, J.C.; Dai, S.; Wang, P.; Xie, P.; Liu, J. Petrology and geochemistry of the Harlan, Kellioka, and Darby coals from the Louellen 7.5-Minute quadrangle, Harlan County, Kentucky. *Minerals* **2015**, *5*, 894–918. [CrossRef]
41. Kravits, C.M.; Crelling, J.C. Effects of overbank deposition on the quality and maceral composition of the Herrin (No.6) coal (Pennsylvanian) of Southern Illinois. *Int. J. Coal Geol.* **1981**, *1*, 195–212. [CrossRef]

42. Hayashi, K.I.; Fujisawa, H.; Holland, H.D.; Ohmoto, H. Geochemistry of 1.9 Ga sedimentary rocks from northeastern Labrador, Canada. *Geochim. Cosmochim. Acta* **1997**, *61*, 4115–4137. [CrossRef]
43. He, B.; Xu, Y.G.; Zhong, Y.T.; Guan, J.P. The Guadalupian–Lopingian boundary mudstones at Chaotian (SW China) are clastic rocks rather than acidic tuffs: Implication for a temporal coincidence between the end-Guadalupian mass extinction and the Emeishan volcanism. *Lithos* **2010**, *119*, 10–19. [CrossRef]
44. Dai, S.; Yang, J.; Ward, C.R.; Hower, J.C.; Liu, H.; Garrison, T.M.; French, D.; O'Keefe, J.M.K. Geochemical and mineralogical evidence for a coal-hosted uranium deposit in the Yili Basin, Xinjiang, northwestern China. *Ore Geol. Rev.* **2015**, *70*, 1–30. [CrossRef]
45. Hower, J.C.; Eble, C.F.; O'Keefe, J.M.K.; Dai, S.; Wang, P.; Xie, P.; Liu, J.; Ward, C.R.; French, D. Petrology, palynology, and geochemistry of Gray Hawk Coal (Early Pennsylvanian, Langsettian) in Eastern Kentucky, USA. *Minerals* **2015**, *5*, 592–622. [CrossRef]
46. Zhao, L.; Ward, C.R.; French, D.; Graham, I.T. Major and trace element geochemistry of coals and intra-seam claystones from the Songzao Coalfield, SW China. *Minerals* **2015**, *5*, 870–893. [CrossRef]
47. Gould, K.W.; Smith, J.W. The genesis and isotopic composition of carbonates associated with some Permian Australian coals. *Chem. Geol.* **1979**, *24*, 137–150. [CrossRef]
48. Dai, S.; Ren, D.; Tang, Y.; Shao, L.; Li, S. Distribution, isotopic variation and origin of sulfur in coals in the Wuda coalfield, Inner Mongolia, China. *Int. J. Coal Geol.* **2015**, *51*, 237–225. [CrossRef]
49. Chen, Z.H.; Wu, F.D.; Zhang, S.L.; Zhang, N.M.; Ma, J.X.; Ge, L.G. *Sedimentary Environments and Coal Accumulation of Late Paleozoic Coal Formation in Northern China*; Press of China University of Geosciences: Beijing, China, 1993; p. 190. (In Chinese)
50. Lan, X.H.; Ma, D.X.; Xu, M.G. Some geochemical indicators of the Pearl River Delta and their facies significance. *Mar. Geol. Quat. Geol.* **1987**, *7*, 39–49. (In Chinese)
51. Chen, Z.; Chen, Z.; Zhang, W. Quaternary stratigraphy and trace-element indices of the Yangtze Delta, Eastern China, with special reference to marine transgressions. *Quat. Res.* **1997**, *47*, 181–191. [CrossRef]
52. Chagué-Goff, C. Chemical signatures of palaeotsunamis: A forgotten proxy? *Mar. Geol.* **2010**, *271*, 67–71. [CrossRef]
53. Bouška, V.; Pešek, J.; Sykorova, I. Probable modes of occurrence of chemical elements in coal. *Acta Montana Ser. B Fuel Carbon Mineral Process. Praha* **2000**, *10*, 53–90.
54. Dai, S.; Chou, C.-L. Occurrence and origin of minerals in a chamosite-bearing coal of Late Permian age, Zhaotong, Yunnan, China. *Am. Mineral.* **2007**, *92*, 1253–1261. [CrossRef]
55. Kolker, A.; Chou, C.-L. Cleat-filling calcite in Illinois Basin coals: Trace element evidence for meteoric fluid migration in a coal basin. *J. Geol.* **1994**, *102*, 111–116. [CrossRef]
56. Shields, A.J. Secondary Mineralization in Coal: Case Study of the Bunnerong PHKB 1 Borehole, Sydney Basin, Australia. Unpublished. Bachelor's (Honours) Thesis, University of Sydney, Sydney, Australia, 1994. p. 101.
57. Dai, S.; Chou, C.-L.; Yue, M.; Luo, K.; Ren, D. Mineralogy and geochemistry of a Late Permian coal in the Dafang Coalfield, Guizhou, China: Influence from siliceous and iron-rich calcic hydrothermal fluids. *Int. J. Coal Geol.* **2005**, *61*, 241–258. [CrossRef]
58. Dai, S.; Liu, J.; Ward, C.R.; Hower, J.C.; French, D.; Jia, S.; Hood, M.M.; Garrison, T.M. Mineralogical and geochemical compositions of Late Permian coals and host rocks from the Guxu Coalfield, Sichuan Province, China, with emphasis on enrichment of rare metals. *Int. J. Coal Geol.* **2016**. [CrossRef]